5 Materials Science

5-1 Ferroelectricity in (Tb,Dy)MnO_3 Derived from Spiral Spin Ordering

Strong coupling between ferroelectricity and magnetic order has attracted much interest since Kimura *et al.* reported a magnetic-field-induced flop of electric polarization from the *c* to *a* direction in $TbMnO_3$ and $DyMnO_3$ [1,2]. This unique magnetoelectric effect is ascribed to a magnetic-field-induced phase transition in geometrically frustrated Mn-spin systems [3]. In fact, our synchrotron X-ray diffraction study indicates that application of magnetic fields causes an abrupt change in antiferromagnetic structure upon the polarization flop [4]. Some magnetic structures in geometrically frustrated systems generate macroscopic electrical polarization, while others do not. In earlier studies, ferroelectricity was considered to arise from the incommensurate-commensurate transition in antiferromagnetic Mn-spin order [1,2]. However, it has been pointed out that transverse spiral spin ordering, in which the spiral axis is perpendicular to the propagation vector, can also induce ferroelectric polarization regardless of the commensurability between the spin modulation and the crystal lattice. According to Katsura *et al.* [5], the position of the oxygen ion between the two magnetic ions (M_1 and M_2) can be affected by the vector product of the two magnetic moments, $\boldsymbol{S}_i \times \boldsymbol{S}_j$ (see Fig. 1(a)). Since the vector product of any two neighboring Mn moments is almost uniform in transverse spiral ordering, all the oxygen ions are displaced in the same direction and hence ferroelectric polarization emerges, as shown in Fig. 1(b). This mechanism is closely related to the antisymmetric superexchange or the so-called Dzyaloshinsky-Moriya (DM) interaction [6,7]. A bending M_1-O-M_2 bond lacking an inversion center favors a canted spin arrangement. This antisymmetric superexchange interaction is expressed as $\boldsymbol{D}\cdot\boldsymbol{S}_i \times \boldsymbol{S}_j$, where the DM vector $\boldsymbol{D}$ depends on the displacement of the intermediate oxygen.

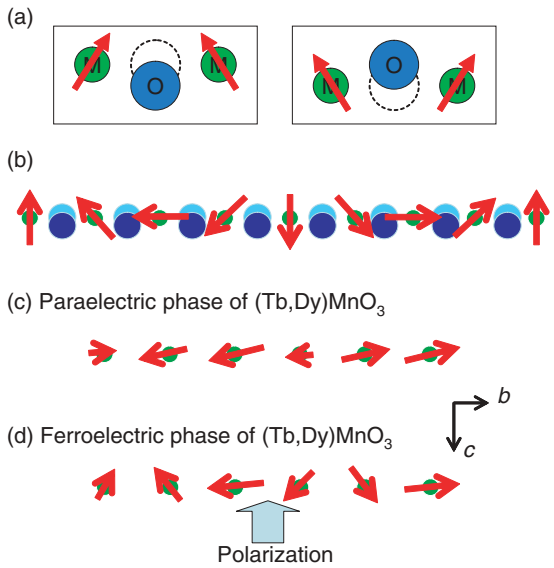

Figure 1
(a) The position of the oxygen ion between the two magnetic ions is affected by the vector product of the two magnetic moments. (b) Transverse spiral spin order moves each oxygen ion in the same direction. (c) In the paraelectric phase the Mn spin moments are sinusoidally almost aligned in the *b* direction. (d) At lower temperatures the Mn spin moments align in a transverse spiral (elliptical) form, producing macroscopic polarization along the *c* axis.

In order to clarify the origin of the ferroelectricity, we performed synchrotron X-ray and neutron diffraction studies on magnetic structures in (Tb,Dy)MnO_3 [8]. Off-resonant synchrotron X-ray diffraction measurements in $RMnO_3$ with various rare earth elements *R* were carried out at BL-4C. The superlattice modulation wavenumber was deduced from the superlattice reflection position and is plotted as a function of temperature in Fig. 2. The ferroelectric transition temperature for each compound is indicated by an arrow. The modulation vector is common and independent of temperature in both the paraelectric and the ferroelectric phases in (Tb,Dy)MnO_3. It is well known that the superlattice modulation vector is twice as large as the propagation vector of the antiferromagnetic order. As a consequence, in (Tb,Dy)MnO_3 we conclude that the ferroelectricity in these compounds is irrelevant to the commensurability of antiferromagnetic spin order.

The magnetic structure in the paraelectric and ferroelectric phases of $Tb_{0.63}Dy_{0.37}MnO_3$ below the Néel temperature (~40 K) was deduced from single-crystal

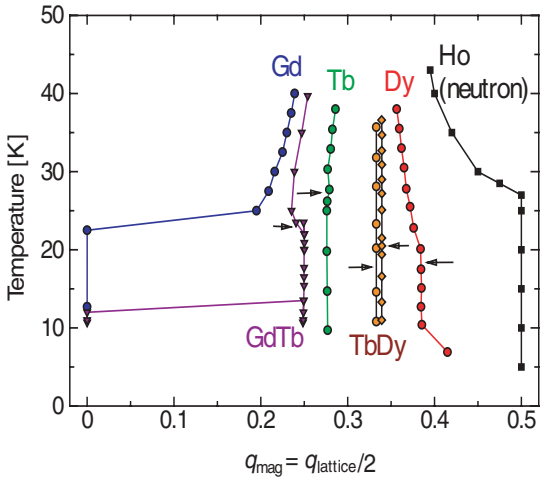

Figure 2
Modulation wavenumber in Mn spin (q_{mag}) and lattice ($q_{lattice}=2q_{mag}$) system of perovskite manganites $RMnO_3$ as a function of temperature for various rare-earth element *R*. Magnetic modulation vector is described as $\boldsymbol{Q}=(0, q_{mag}, 1)$. GdTb denotes $Gd_{0.7}Tb_{0.3}$. Two sets of data of TbDy are for $Tb_{0.50}Dy_{0.50}$ and $Tb_{0.32}Dy_{0.68}$. Arrows indicate ferroelectric transition temperatures.

neutron diffraction data collected using a neutron four-circle diffractometer FONDER at JRR-3M, Japan [8]. The obtained magnetic structures are schematically shown in Figs. 1(c) and (d). The almost collinear alignment of Mn spin moments observed in the paraelectric phase changes to transverse spiral ordering upon the ferroelectric transition. We have clearly shown that the ferroelectricity in (Tb,Dy)MnO_3 has its origin in transverse spiral ordering in Mn spin moments.

T. Arima[1,2,3], A. Tokunaga[3], T. Goto[4], H. Kimura[1], Y. Noda[1] and Y. Tokura[2,4] (Tohoku Univ., [2]ERATO-SSS, Japan Sci. & Tech. Agency, [3]Univ. of Tsukuba, [4]The Univ. of Tokyo)

References

[1] T. Kimura, T. Goto, H. Shintani, K. Ishizaka, T. Arima and Y. Tokura, *Nature,* **426** (2003) 55.
[2] T. Goto, T. Kimura, G. Lawes, A. P. Ramirez and Y. Tokura, *Phys. Rev. Lett.*, **92** (2004) 257201.
[3] T. Kimura, S. Ishihara, H. Shintani, T. Arima, K. T. Takahashi, K. Ishizaka and Y. Tokura, *Phys. Rev. B*, **68** (2003) 060403(R).
[4] T. Arima, T. Goto, Y. Yamasaki, S. Miyasaka, K. Ishii, M. Tsubota, T. Inami, Y. Murakami and Y. Tokura, *Phys. Rev. B,* **72** (2005) 100102(R).
[5] H. Katsura, N. Nagaosa and A. V. Balatsky, *Phys. Rev. Lett.,* **95** (2005) 057205.
[6] I. Dzyaloshinsky, *J. Phys. Chem. Solids,* **4** (1958) 241.
[7] T. Moriya, *Phys. Rev.,* **120** (1960) 91.
[8] T. Arima, A. Tokunaga, T. Goto, H. Kimura, Y. Noda and Y. Tokura, *Phys. Rev. Lett.*, **96** (2006) 097202.

5-2 Antiferro Orbital Ordering in a Mn Oxide Thin Film

Charge order and orbital order (CO/OO) are characteristic phenomena of correlated electron systems. Manganese oxides are good examples of such systems since they display various ground states and complicated interplay of the charge, spin and orbital degrees of freedom [1]. Control of the ferro-orbital ordering has been achieved by utilizing the thin film technique [2], manipulating the in-plane strain in the specimens. Although a number of films have been fabricated on cubic perovskite (001) substrates, none have shown a first-order metal-insulator transition [3], which is often observed in bulk Mn oxides at the CO/OO transition temperature. The strong coupling between the orbital and lattice degrees of freedom which enables control of the ferro-orbital ordering is thought to prevent a sharp phase transition to the OO phase. It has been reported [4] that $Nd_{0.5}Sr_{0.5}MnO_3/SrTiO_3$(011) shows a sharp first-order phase transition around 170 K (T_{MI}); the resistivity as a function of temperature observed for this sample is shown in Fig. 3(a). We have studied the OO in this new system with the (011) substrate by making X-ray diffraction measurements in order to clarify what modes of lattice distortion are required for the metal-insulator transition [5].

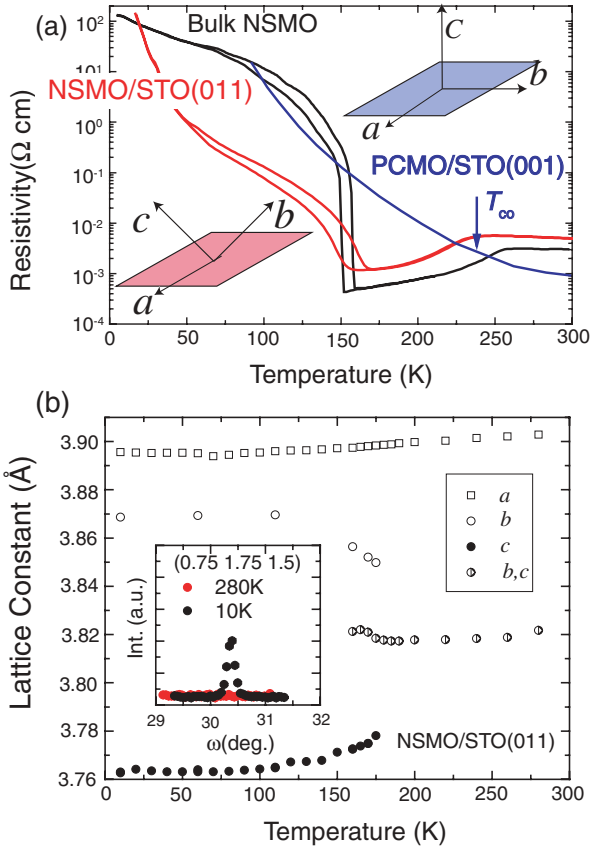

Figure 3
(a) Electric resistivity of $Nd_{0.5}Sr_{0.5}MnO_3/SrTiO_3$(011) [4], $Pr_{0.5}Ca_{0.5}MnO_3/SrTiO_3$(001) [3] and bulk $Nd_{0.5}Sr_{0.5}MnO_3$ [6] as functions of temperature. (b) Temperature dependence of the lattice parameters of $Nd_{0.5}Sr_{0.5}MnO_3/SrTiO_3$(011) measured at BL-4C. The inset shows the intensity distribution around the (3/4 7/4 3/2) superlattice position at 10 K and 280 K. A sharp peak was observed below150 K.

The X-ray diffraction experiments were carried out at BL-4C and BL-16A2. These beamlines are equipped with standard four-circle diffractometers with closed-cycle refrigerators. Epitaxial films were grown by the pulsed-laser deposition method to thicknesses of 80 nm. Our experimental results, presented in Fig. 3(b), show a drastic change in the lattice parameters at the metal-insulator transition temperature of 170 K, as well as the appearance of superlattice reflections below 150 K. The lattice parameters observed are similar to those for bulk crystals. The low-temperature lattice parameters characterized by $a \sim b > c$ are in good agreement with those associated with x^2-y^2- type ferro OO and $3x^2-r^2/3y^2-r^2$-type antiferro OO.

Based on the position of the superlattice reflections, the size of the unit cell below 150 K was found to be $\sqrt{2}\times2\sqrt{2}\times2$ times as large as that of the $SrTiO_3$ unit cell. Measuring a large number of superlattice reflections, we have deduced a CE-type orbital-ordered structure shown in Fig. 4, whereas the structure between 150 K and 170 K is an x^2-y^2- type ferro OO. This is the first observation of an antiferro OO in manganite epitaxial thin films; using (011) substrates allows a lattice distortion that decreases the free energy of the antiferro OO while (001) substrates prohibit it. This result provides a clue

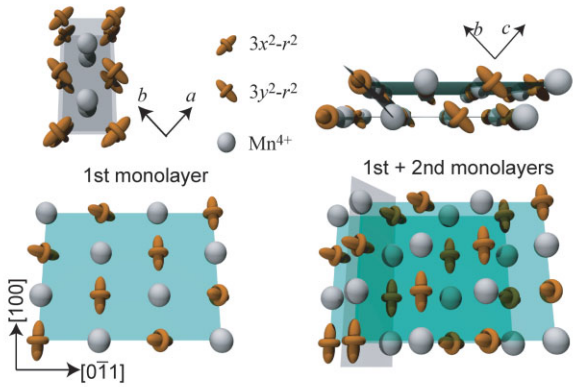

Figure 4
Schematic view of the orbital order structure in the Mn oxide thin film on $SrTiO_3$ (011) substrate. White spheres represent the Mn^{4+} ions, orange symbols the Mn^{3+} ions, and the c- and (011)- planes are displayed in grey and green, respectively.

to the possible modes of distortion that directly relate to the antiferro OO. For example, (a) shrinkage of the c-lattice constant without any large change in cell volume, and (b) causing different lengths of a+b and a-b (i.e., lattice parameters a and b in $\sqrt{2}\times\sqrt{2}\times2$ orthorhombic cell). This result shows that studying thin films provides much information about the relation between the lattice strain and the orbital ordering, which couples closely to the electron correlation.

Y. Wakabayashi[1], D. Bizen[2], H. Nakao[2], Y. Murakami[2,3], M. Nakamura[4], Y. Ogimoto[5], K. Miyano[4] and H. Sawa[1] ([1]KEK-PF, [2]Tohoku Univ. [3]JAERI, [4]The Univ. of Tokyo, [5]SHARP Cor.,)

References

[1] Y. Tokura and N. Nagaosa, *Science,* **288** (2000) 462.
[2] Y. Konishi, Z. Fang, M. Izumi, T. Manako, M.Kasai, H. Kuwahara, M. Kawasaki, K. Terakura and Y. Tokura, *J. Phys. Soc. Jpn.*, **68** (1999) 3790.
[3] W. Prellier, Ch. Simon, A. M. Haghiri-Gosnet, B. Mercey and B. Raveau, *Phys. Rev. B,* **62** (2000) R16337.
[4] Y. Ogimoto, M. Nakamura, N. Takubo, H. Tamaru, M. Izumi and K. Miyano, *Phys. Rev. B,* **71** (2005) 060403(R).
[5] Y. Wakabayashi, D. Bizen, H. Nakao, Y. Murakami, M. Nakamura, Y. Ogimoto, K. Miyano and H. Sawa, *Phys. Rev. Lett.,* **96** (2006) 017202.
[6] Y. Tokura, H. Kuwahara, Y. Moritomo, Y. Tomioka and A. Asamitsu, *Phys. Rev. Lett.*, **76** (1996) 3184.

5-3 Photo-Induced Effects in Quantum Paraelectric $SrTiO_3$ Probed by X-Ray Absorption Spectroscopy

The study of photo-induced phase transitions is of great importance not only in the basic fields of non-equilibrium physics but also for the invention of new devices. $SrTiO_3$ has a quantum paraelectricity (QPE) below 105 K due to the competition between quantum fluctuations and cooperative dipole-dipole interaction. Unique photo-induced effects such as self trapped exitons [1], gigantic photo-induced dielectric constants [2] and giant photo conductivity [3] have recently been observed in QPE-phase $SrTiO_3$. The pre-edge peak in Ti K-edge X-ray absorption near edge structure (XANES) spectra is very sensitive to the inversion symmetry at a Ti-atom site and changes in electronic state. Thus XANES is a powerful tool for exploring the detailed electronic structure of $SrTiO_3$ influenced by photo-induced effects.

Photo-induced XANES spectra have been recorded at the Ti-K edge in $SrTiO_3$ utilizing BL-9A. The sample was a 10 × 10 × 1 mm^3 single crystal of $SrTiO_3$. A Hg-Xe lamp with a heat-ray-cutting filter was used as a UV source, providing an output power of 5 mW/cm^2 at the sample.

The red trace of Fig. 5 shows the Ti K-edge XANES spectrum recorded at 12 K. Three well-resolved pre-peaks (A1, A2 and A3) are observed. Judging from the azimuthal-angular dependence, the A1 and A2 peaks can be attributed to electric-quadrupole transitions associated with excitations from the 1s-core to the 3d(t_{2g}) (A1) and 3d(e_g) (A2) valence states. The azimuthal-angular dependence of the intensity of the A3 peak shows that it can be attributed to an electric-dipole transition.

The blue trace of Fig. 5 shows the photo-induced XANES spectrum recorded at 12 K. Under UV irradiation only the intensity of peak A2 increases (arrow). The inset of Fig. 5 shows the intensity of the A2 peak plotted against time, with UV irradiation taking place between 0 min and 30.5 min. The observed lifetime of the change in the spectrum induced by UV irradiation was about 10 min. This photo-induced effect was observed only in the QPE phase and not in the high-temperature phase. A theoretical calculation indicates that the increase in intensity of only the A2 peak arises from the displacement of Ti atoms toward the oxygen atoms. Moreover, in the extended X-ray absorption fine structure (EXAFS) region, the period of the EXAFS oscillations does not change under UV irradiation, but the EXAFS amplitude

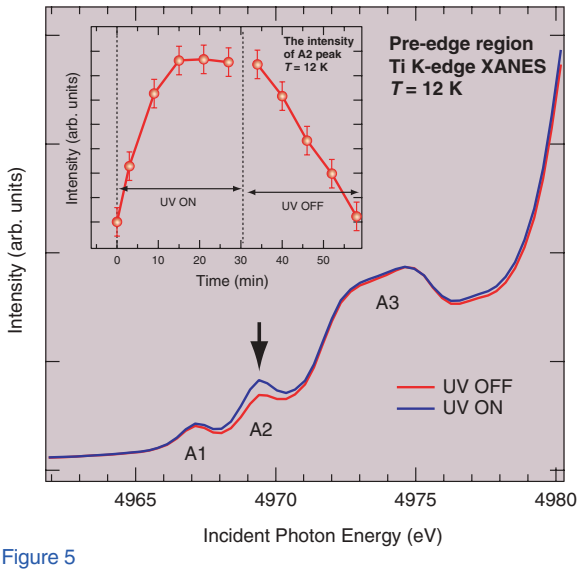

Figure 5
The photo-induced effect in the pre-edge region of Ti K-edge XANES. The inset shows the intensity of peak A2 plotted against time.

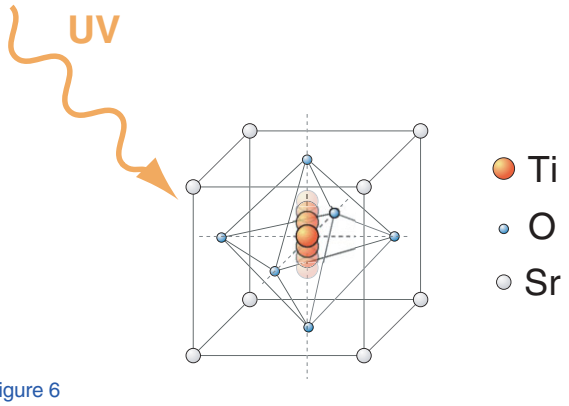

Figure 6
Schematic representation of the local vibration excited by UV irradiation in the QPE phase.

slightly increases with UV irradiation (not shown here). Thus, it is concluded that vibrations along the direction of the Ti-O bond are excited by UV irradiation.

A schematic representation of the uniaxial photo-induced vibration at the Ti atom is given in Fig. 6. This photo-induced behavior can be explained by a fluctuation of the inversion symmetry accompanied by local vibrations of the Ti atoms excited by UV irradiation. Therefore, the result of the photo-induced X-ray absorption experiment clearly shows that the ferroelectric fluctuation has been enhanced in photo-irradiated QPE systems. The full results of the present experimental study are published in [4].

S. Nozawa[1], T. Iwazumi[1] and H. Osawa[2] ([1]KEK-PF, [2]Grad. Univ. for Adv. Stud.)

References

[1] T. Hasegawa, M. Shirai and K. Tanaka, *J. Lumin.,* **87** (2000) 1217.
[2] M. Takesada, T. Yagi, M. Itoh and S. Koshihara, *J. Phys. Soc. Jpn.*, **72** (2003) 37.
[3] T. Ishikawa, M. Kurita, H. Shimoda, Y. Sakano, S. Koshihara, M. Itoh and M. Takesada, *J. Phys. Soc. Jpn.*, **73** (2004) 1635.
[4] S. Nozawa, T. Iwazumi and H. Osawa, *Phys. Rev. B,* **72** (2005) 121101.

5-4 Co-Existing Handednesses of Lamella Twisting in a Spherulite of Polymer Blend

It is well known that some polymer crystals form twisting lamella structures when they grow from the center of a spherulite, and that spherulites with banding patterns (banding spherulites) can be observed using a polarized optical microscope (POM) in such polymers due to the periodic change of the direction of the index ellipsoid. The origin of this twisting has been widely investigated and discussed [1,2]. Mechanisms such as main chain chirality and asymmetric stress at the growth front have been suggested. When considering the origin of such lamella twisting, handedness is one of the most important ingredients since it is expected to be strongly related to the twisting mechanism. When the origin of twisting is chirality in the main chains of the polymer, the chiral nature may relate to the handedness of the lamella twisting. On the other hand, when the twisting originates in the asymmetry of stress at the growth front (such as the main chain tilt), handedness is likely to be random.

Poly(ε-caprolacton) (PCL)/poly(vinyl butyral) (PVB) blend is known as a blend system which forms a large spherulite (diameter of around 1-2 mm for 40°C isothermal crystallization) with highly ordered banding [3]. It is considered that the hydrogen-bonding interaction between PCL and PVB is the origin of suppression in the nucleation rate, resulting in the formation of a large spherulite. With respect to the driving force to form a twisting lamella structure in PCL/PVB, neither of which have chiral structures in the main chains, it is reasonable to think that there exists some form of asymmetric stress at the growth front of the PCL crystal due to the inhomogeneous distribution of PVB. In PCL/PVB, some straight lines along the radial direction of the spherulite are observed under POM (Fig. 7), which are also observed in some of other band spherulites [4]. By using microbeam-scanning wide-angle X-ray scattering (WAXS), we have investigated the origin of the straight line and its relation to the handedness of lamella twisting [5].

PCL and PVB supplied by Polysciences Inc. (Warrington, PA) were used as received. The molecular weight of PCL was 65,000 and that of PVB was 100,000. The PCL/PVB blend sample was prepared by dissolving PCL and PVB in the common solvent tetrahydrofuran with a blend ratio of 95/5. The obtained PCL/PVB blend sample was pressed to a thickness of 20-30 μm and isothermally crystallized at 40ºC. The microbeam WAXS experiment was performed at BL-4A [6]. The X-ray beam was focused to 4×4 μm^2 at the sample position with a Kirkpatrick-Baez mirror. We scanned the spherulite along the left- and right-side of the lines with the microbeam with a step size of 1 μm and measured the periodic change of the azimuthal angle of 110 reflection positions in the WAXS. In Fig. 8, the sequences

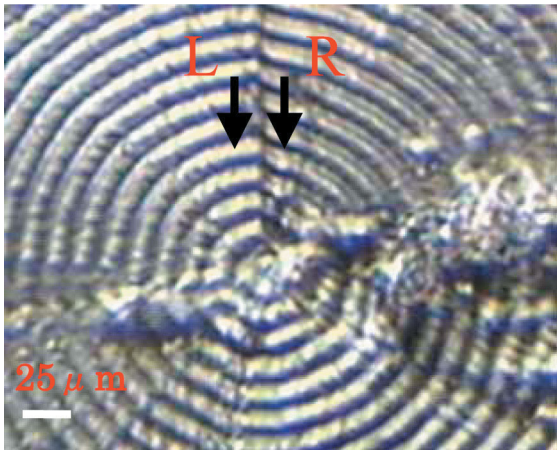

Figure 7
POM image of PCL/PVB banding spherulite. Straight lines radiating from the center are observed. The location of the region scanned with the microbeam is also indicated.

of the azimuthal intensity distribution of 110 reflections at the left (L) and right (R) sides of the straight line are shown as contour maps, in which the azimuth angle is taken as abscissa and the microbeam position as ordinate. From Fig. 8, we have observed that the manner of the periodic change of the 110 reflection in WAXS is clearly inverse between the left and right sides of the straight line with respect to the direction of the X-ray beam scanning. This result clearly indicates that the straight line observed under POM is the 'boundary line' of handedness in a band spherulite, and further that both handednesses co-exist within 'one' spherulite. This coexistence of handedness also indicates that the lamellae growing from a nucleus of a spherulite are twisted cooperatively only with neighboring lamellae, and not with all lamellae from the nucleus.

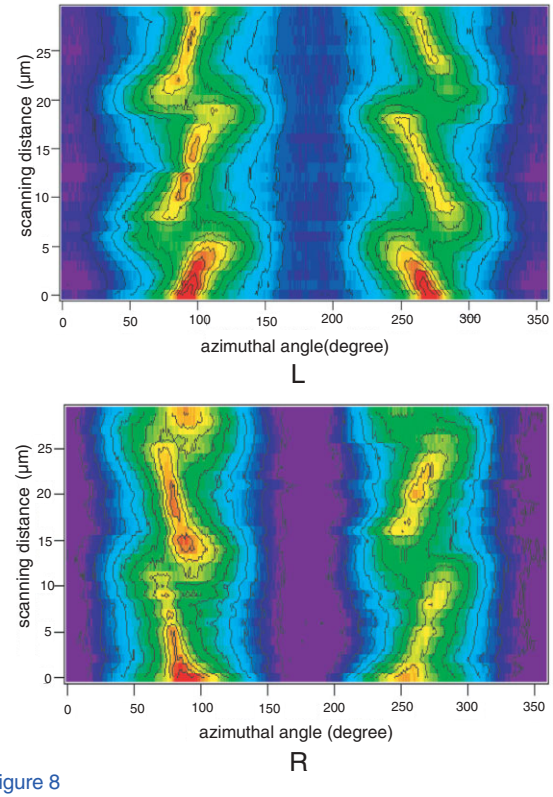

Figure 8
Intensity contour maps of the 110 reflection azimuthal distribution in WAXS using an X-ray microbeam scanning L line (upper) and R line (lower) of the PCL/PVB band spherulite shown in Fig. 7.

Y. Nozue[1], N. Kawasaki[2], R. Kurita[2], A. Iida[3] and Y. Amemiya[2] ([1]Sumitomo Chem. Japan, [2]The Univ. of Tokyo [3]KEK-PF)

References

[1] H. D. Keith and F. J. Padden, Jr., *Macromolecules*, **29** (1996) 7776.
[2] K. L. Singfield, J. M. Klass and G. R. Brown, *Macromolecules,* **28** (1995) 8006.
[3] H. D. Keith, F. J. Padden, Jr. and T. P. Russell, *Macromolecules,* **22** (1989) 666.
[4] Y. Jiang, J. J. Zhou, L. Li, J. Xu, B. H. Guo, Z. M. Zhang, Q. Wu, G. Q. Chen, L. T. Weng, Z. L. Cheung and C. M. Chan, *Langmuir,* **19** (2003) 7417.
[5] Y. Nozue, S. Hirano, R. Kurita, N. Kawasaki, S. Ueno, A. Iida, T. Nishi and Y. Amemiya, *Polymer,* **45** (2004) 8299.
[6] A. Iida and T. Noma, *Nucl. Instrum. Meth.* Phys. Res. B, **82** (1993) 129.

5-5 Intralayer Molecular Orientation in the B1 Phase of a Bent-Core Liquid-Crystal Molecule Studied by X-Ray Micro-Beam Diffraction

Achiral bent-core liquid crystals are very interesting from the viewpoint of "*chirality*" appearing in an "*achiral*" molecular system [1], and have been investigated experimentally and theoretically by many researchers. Bent-core molecules exhibit specific mesogenic phases, B1~B8, different from those in rod-like molecules. The determination of the structure in each phase is crucial but not easy due to the difficulties in obtaining large uniform domains. The B1 phase was found in P-6-O-PIMB (Fig. 9(a)) [2]. A two-dimensional (2D) modulated structure (Col(*p2mg*)), shown in Fig. 9(b), has been proposed for this phase based on macroscopic X-ray diffraction studies. On the other hand, another 2D structure (Col($pm2_1m$)), shown in Fig. 9(c), has been very recently proposed for other compounds [3].

In order to determine precisely the molecular orientation in the B1 phase, X-ray micro-beam-diffraction measurements were carried out at BL-4A, and the relation between the layer structure and the intralayer molecular orientation are discussed. The sample used was P-6-O-PIMB (see Fig. 9(a)), sandwiched between two 80-μm-thick glass plates coated with an ITO electrode. The cell gap was 29 μm. We were able to obtain relatively large uniform B1 domains, as shown in Fig. 10(a), by gradually cooling from the isotropic liquid. The X-ray energy was 14 keV and the beam size was 3×4 μm^2 [4]. A CCD camera with an image intensifier was used as a 2D detector.

Figure 10(b) shows the 2D X-ray profiles at small and wide angles before applying an electric field. At small angles, only one pair of (002) spots was observed. The corresponding spacing (19.3 Å) is almost equivalent to half of the molecular length. At wide angles, four diffuse peaks were observed symmetrically with respect to (002) spots, and the angle between them, 36.7°, is close to the supplementary angle of the molecular bending angle of 132.3° (see Fig. 9(a)). Figure 10(f) shows the 2D X-ray profiles at small and wide angles obtained from the same irradiated spot under the application of a DC electric field. At small angles, two additional pairs of spots with a spacing of 29.1 Å appear symmetrically with respect to the (002) spots. At the wide angles, the diffuse-scattering pattern also changes to two peaks. This pattern arises from the 2D modulated structure, and the additional spots correspond to (101). Considering that the powder X-ray diffraction results exhibit (002) and (101) diffraction peaks regardless of the applied field [2,3], we conclude that this change in diffraction pattern is not caused by a structural change, but by a layer (or molecular) orientation change. Our result in-

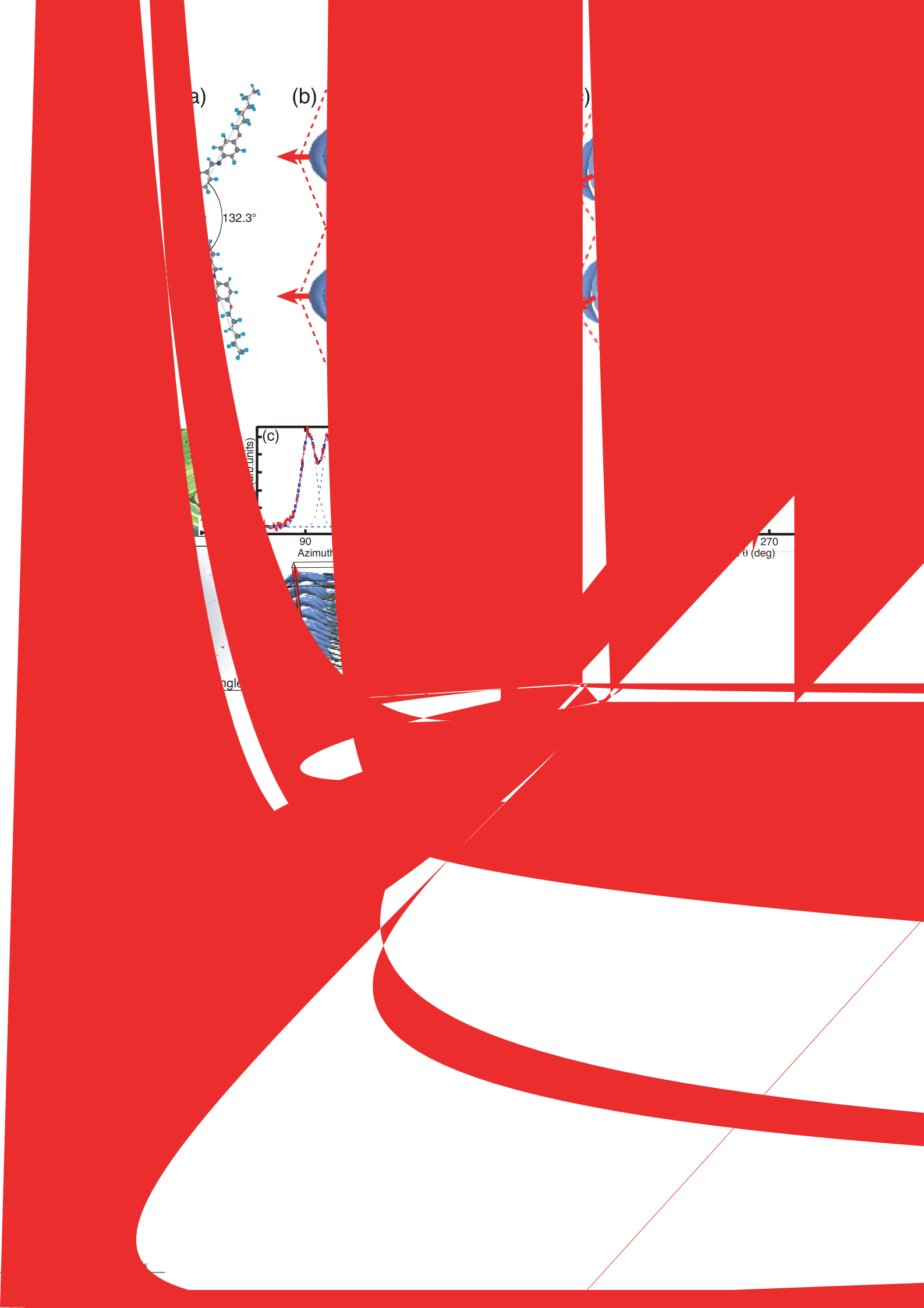
a)
(b)
132.3°
(c)
90
270
θ (deg)